

Dear editors and reviewer:

Thank you for your comments concerning our manuscript entitled “The interaction between urbanization and aerosols during the typical haze event”. The comments are all valuable for improving the manuscript and also have great guiding significance for our research. We have studied the comments carefully and made corrections that we hope will be met with your approval. One version of the revised manuscript is highlighted with Track Changes. In the following we quoted each review question and added our response after each paragraph.

Reviewer #2:

The authors investigate the interaction between aerosols and urbanization during a severe haze event via the RMAPS-ST model. Results indicate that a 100% increase in PM2.5 (200 to 400 $\mu\text{g}\cdot\text{m}^{-3}$) reduced daytime urban-related warming by 20% (from 30-50%). However, urban-related warming increased approximately 28% in response to aerosols- important for haze formation. With regards to urbanization, the aerosol-related cooling effect was reduced by approximately 54%, changing little with aerosol increases. The study also found that aerosols reduced the urban-impact on the mixing layer, sensible heat flux, and latent heat flux by 148%, 156%, and 48.8%, respectively. In their revision, the authors appropriately addressed the reviewer suggestions and created an improved manuscript. This reviewer suggests minor changes as follows:

- 1) *Change the title to: “The interaction between urbanization and aerosols during a typical winter haze event in Beijing.”*

The suggested change has been made.

- 2) *Rephrase Lines 29-32: “The effects of urbanization and aerosols were investigated during a typical winter haze event. The event, which occurred in Beijing from 15-22 December 2016, was studied via the rapid-refresh multiscale analysis and prediction system-short term (RMAPS-ST) model.”*

The suggested change has been made.

3) *Rephrase from Line 34: “Aerosols reduced urban-related warming during the daytime by 20% (from 30 to 50%) as PM2.5 concentrations increased from 200 to 400 $\mu\text{g}\cdot\text{m}^{-3}$.”*

The suggested change has been made.

4) *Rephrase from Line 99: ”Cao et al. (2016) describes the first attempt to determine...”*

The suggested change has been made.

5) *Rephrase Lines to 269-271 and add to the previous paragraph.*

The revised the sentence in Lines 276-269: It was not until the strong cold air moved southward in the early morning of the 22nd when the whole atmosphere converted to the northwest stream. The air pollutants were completely removed in the third stage.

6) *Line 356: replace “smaller” with “less”.*

The suggested change has been made.

7) *Paragraph starting from Line 430: Break into two paragraphs, perhaps from line 441.*

The suggested change has been made.

1 **The interaction between urbanization and aerosols during a typical winter haze**
2 **event in Beijing**

3 ~~**The interaction between urbanization and aerosols during a haze event**~~

4

5

6 Miao Yu¹, Guiqian Tang², Yang Yang¹, Qingchun Li¹, Yonghong Wang², Shiguang
7 Miao¹, Yizhou Zhang¹, Yuesi Wang²

8

9

10 1. *Institute of Urban Meteorology, China Meteorological Administration, Beijing, China*
11 2. *State Key Laboratory of Atmospheric Boundary Layer Physics and Atmospheric Chemistry
12 (LAPC), Institute of Atmospheric Physics, Chinese Academy of Sciences, Beijing 100029,
13 China*

14

15

16

17

18 *Submitted to Atmospheric Chemistry and Physics*

19

20

21

22

23 *Corresponding author:*

24 Guiqian Tang

25 *State Key Laboratory of Atmospheric Boundary Layer Physics and Atmospheric Chemistry
26 (LAPC), Institute of Atmospheric Physics, Chinese Academy of Sciences, Beijing 100029, China*

27

Abstract

29 Aerosols cause cooling at the surface by reducing shortwave radiation, while
30 urbanization causes warming by altering the surface albedo and releasing
31 anthropogenic heat. The combined effect of the two phenomena needs to be studied in
32 depth. The effects of urbanization and aerosols were investigated during a typical winter
33 haze event. The event, which occurred in Beijing from 15-22 December 2016, was
34 studied via the rapid-refresh multiscale analysis and prediction system-short term
35 (RMAPS-ST) model. The interaction between aerosols and urbanization during the haze
36 event that occurred from the 15th to 22nd of December 2016 in Beijing was investigated
37 using the rapid refresh multiscale analysis and prediction system short term (RMAPS-
38 ST).— The mechanisms of the impacts of aerosols and urbanization were analyzed and
39 quantified. Aerosols reduced urban related warming during the daytime. The urban-
40 related warming decreased by 30 to 50% as the concentration of PM_{2.5} increased from
41 200 to 400 $\mu\text{g}\cdot\text{m}^{-3}$. Aerosols reduced urban-related warming during the daytime by 20%
42 (from 30 to 50%) as PM_{2.5} concentrations increased from 200 to 400 $\mu\text{g}\cdot\text{m}^{-3}$.
43 Conversely, aerosols also enhanced urban-related warming at dawn, and the increment
44 was approximately 28%, which contributed to haze formation. Urbanization reduced
45 the aerosol-related cooling effect by approximately 54% during the haze event, and the
46 strength of the impact changed little with increasing aerosol content. The impact of
47 aerosols on urban-related warming was more significant than the impact of urbanization
48 on aerosol-related cooling. Aerosols decreased the urban impact on the mixing layer
49 height by 148% and on the sensible heat flux by 156%. Furthermore, aerosols decreased
50 the latent heat flux; however, this reduction decreased by 48.8% due to urbanization.
51 The impact of urbanization on the transport of pollutants was more important than that
52 of aerosols. The interaction between urbanization and aerosols may enhance the
53 accumulation of pollution and weigh against diffusion.

1 Introduction

56 In recent years, heavy haze pollution events have increasingly occurred in densely

57 populated urban areas, such as the Beijing-Tianjin-Hebei region (BTH region) and
58 Yangtze River Delta region of China (Zhang et al., 2019). These events have caused
59 increasingly severe adverse effects on transportation, the ecological environment and
60 human health (Zhao et al., 2012; Wu et al., 2010; Liu et al., 2012). A statistical analysis
61 of the variation in haze days in Beijing over the past 10 years showed that the number
62 of haze days has significantly increased (Chen and Wang, 2015; Zhai et al., 2019). The
63 average annual number of haze days was 162 from 1981-1990, 167 from 1991-2000,
64 and 188 from 2001-2010. The conditions for the formation of heavy haze in the BTH
65 region are very complex (Miao et al., 2017; Wei et al., 2018; Ren et al., 2019). Although
66 emissions, meteorological conditions, terrain, and high-density human activities in
67 urban areas are all important conditions for the evolution of heavy haze (Huang et al.,
68 2008a; Zhu et al., 2018), meteorological conditions are critical for the evolution of
69 heavy haze pollution weather under the background of constant emissions (Wang et al.,
70 2020; Pei et al., 2020).

71
72 The characteristics of the atmospheric boundary layer structure determine the
73 horizontal fluidity, vertical diffusion ability, stability and capacity (mixed layer
74 thickness) of the atmosphere, which are the main factors affecting the formation,
75 intensity and duration of haze and atmospheric pollution (Guo et al., 2016). Coulter R
76 L. (1979) indicated that the height of the mixing layer would affect the concentration
77 and diffusion of pollutants, which has been one of the most important physical
78 parameters in atmospheric numerical models and atmospheric environment evaluations,
79 and urbanization and aerosols have been indicated to influence the boundary layer
80 height (Tao et al., 2015).

81
82 Urbanization, as the most drastic means by which human activities transform the
83 environment, has had an important impact on regional climate and weather processes
84 (Miao et al., 2011; Yu and Liu, 2015; Yu et al., 2017). Existing research suggests that
85 there are three main ways by which urbanization influences the climate (Oke, 1982 and

86 1995). The change in land use from natural surfaces to impervious underlying surfaces
87 in association with urbanization alters the surface albedo and roughness, which results
88 in the formation of urban heat islands (UHIs) (Taha, 1997; Folberth et al., 2014). These
89 alterations lead to a change in the surface energy balance and the form of the thermal
90 difference between urban and rural areas and further change the boundary layer
91 structure (Grimmond, 2007; Li and Bou-Zeid, 2013). Second, thermal differences
92 further lead to heat island circulation, which can influence the local circulation of
93 synoptics and the transport of pollutants (Crutzen, 2004). Anthropogenic aerosols and
94 heat from the development of transportation and industry are also important parts of
95 urban impacts on climate (Huang et al. 2008b). However, in contrast to the effects of
96 urbanization, aerosols cause cooling at the surface by reducing shortwave radiation to
97 enhance static stability (Grimmond, 2007; Crutzen, 2004, Huang et al., 2007).
98 Furthermore, aerosols may increase longwave radiation in urban areas because they are
99 likely to absorb and emit more energy than water vapor or greenhouse gases under
100 certain conditions (Jacobson, 1998; Rudich et al., 2007). There have been few studies
101 on the mechanism of the interaction between urbanization and aerosols, although many
102 studies have focused on their respective effects. Accordingly, the interaction between
103 urbanization and aerosols is important for studying regional climate.

104
105 Researchers are increasingly aware of the importance of the interaction between
106 urbanization and aerosols. A very important study by Cao et al. (2016) describes the
107 ~~was the~~ first attempt to determine the effects of aerosols on urbanization and indicated
108 that aerosols can increase the nighttime UHI effect using a climate model. Yang et al.
109 (2020) obtained different results when using observational data to perform similar
110 research in the BTH region.

111
112 More detailed research needs to be performed by combining observational data and
113 modeling because the conclusions may vary depending on the scale (Xu et al., 2019).
114 Other illuminating work with regional models showed that the combined effect of UHIs

115 and aerosols on precipitation depends on synoptic conditions (Zhong et al., 2015).
116 However, for winter haze, Zhong et al. (2017) evaluated the impact of urban areas on
117 air quality and indicated that urbanization can increase ventilation during the daytime
118 and increase aerosol emissions, and these effects outweigh the UHI effect.

119

120 However, very few studies have quantified the individual effects of urbanization-
121 induced UHIs and elevated aerosol emissions on the formation and development of
122 haze in metropolitan areas. A difficulty faced by such studies is that the radiative forcing
123 of aerosols is not a prognostic variable in most climate models (Cao et al. 2016). Some
124 regional models, such as WRF-Chem, can overcome this problem by parameterizing
125 aerosols to aerosol optical depth (AOD) in some specific radiation schemes. Tao et al.
126 (2015) and Zhong et al. (2018) made some progress in this area, and their results also
127 indicated that a regional model could be used as an effective way to study the interaction
128 between urbanization and aerosols. However, a quantitative evaluation of the impacts
129 or urban areas on aerosols and the simultaneous impacts of aerosols on urban impacts
130 in metropolitan areas has not been attempted.

131

132 In this study, the rapid-refresh multiscale analysis and prediction system-short term
133 (RMAPS-ST) was used to investigate the mechanism of the influence of the above two
134 factors during a typical winter haze event. The objectives of this study are 1) to quantify
135 the impacts of urban areas on aerosols and the impacts of aerosols on urbanization and
136 2) to obtain a better understanding of the interaction between urbanization and aerosols
137 and its influence mechanism on the boundary layer structure and haze transmission
138 during a typical winter haze event in the BTH region.

139

140 **2 Methods**

141 **2.1 Observational data**

142 To investigate the interaction between urbanization and aerosols, observation data on
143 basic meteorological elements, air quality, radiation and surface heat flux and the

144 mixing layer height (MLH) are very important to reveal the impact of urbanization and
145 aerosols during haze events.

146

147 The basic meteorological elements were obtained from 309 national basic weather
148 stations in the BTH region and were provided by the China Meteorological
149 Administration (<http://data.cma.cn/>). The locations of the national basic weather
150 stations are shown in Fig 1 (red dots). The mass concentrations of fine particulate matter
151 (PM_{2.5}) were recorded by 251 environmental monitor stations managed by the Ministry
152 of Ecology and Environment of the People's Republic of China
153 (<http://hbk.cei.cn/aspx/default.aspx>) (Fig 1, black dots). We also used radiation and
154 surface heat flux data to analyze the urban surface energy budget obtained from the
155 Beijing meteorological tower (39.97°N, 116.37°E). The tower is 325 m high and is
156 operated by the Institute of Atmospheric Physics (IAP), Chinese Academy of Sciences
157 (CAS). The heat flux data were measured by a fast response eddy covariance sensor
158 system that was sampled at 10 Hz using CR500 (Campbell Scientific Inc., USA). The
159 radiation data were provided by Kipp & Zonen (Netherlands) four-component
160 unventilated CNR1 radiometers. Radiation and surface flux data from 140 m of the
161 tower were used in this study. In addition, the MLH is an important factor affecting
162 pollutant diffusion and is also affected by both urbanization and aerosols. Because the
163 MLH is not a routine observation, we obtained the data from only one site. The MLH
164 and backscattering coefficient were measured by enhanced single-lens ceilometers
165 (Vaisala, CL51, Finland) deployed by the IAP (Tang et al., 2016). Backscattering
166 coefficient profiles were calculated by referencing the attenuation strobe laser LiDAR
167 technique (910 nm), which is cited in Tang et al. (2015).

168

169 **2.2 Model description and experimental design**

170 To investigate the respective effects of urbanization and aerosols and further determine
171 the interaction between urbanization and aerosols, a high-resolution regional model
172 with satisfactory performance is necessary for sensitivity tests. The model used in this

173 study is the latest available version of RMAPS-ST, which was developed by the
174 Institute of Urban Meteorology, China Meteorological Administration. RMAPS-ST is
175 based on the Weather Research and Forecasting (WRF v3.8.1) model (Skamarock et
176 al., 2008) and its data assimilation system (WRFDA v3.8). The simulation domain was
177 centered at 37.0 °N, 105.0 °E and implemented with two nested grids with resolutions of
178 9 and 3 km for two domains (D1 and D2, respectively) (Fig 1a). The model performance
179 was verified, and RMAPS-ST was run operationally (Fan et al., 2018). The assimilation
180 began every three hours, and the assimilated data included automatic meteorological
181 station data, sounding data and radar data when available. The model settings are shown
182 in Table 1. The simulation started at 0000 LST and ran from the 15th to 23rd of
183 December 2016 with hourly outputs.

184

185 The urban impact was represented by a high-resolution (30 m) land use map interpreted
186 from Landsat Thematic Mapper satellite data from 2015 in Beijing. The urban canopy
187 parameters were optimized according to Miao and Chen (2014). The impact of aerosols
188 was represented by adding the hourly distribution of AOD in the Rapid Radiation
189 Transfer Model for General Circulation Models (RRTMG) radiation scheme. The AOD
190 was extracted from the output of RMAPS-Chem (Zhao et al., 2019; Zhang et al., 2018)
191 for the BTH region, which is shown in Fig 1b. Anthropogenic emission data were
192 obtained according to the Multiresolution Emission Inventory for China (2012)
193 (<http://www.meicmodel.org/>) with a resolution of 0.1°×0.1°. The particle size
194 distribution and typology of aerosols used in this study is according to Ruiz et al. (2014).
195 The simulated distribution of AOD in Beijing was verified to be satisfactory after
196 comparison with the observed vertical profile of the backscattering coefficient (Fig 2a
197 and b). The correlation between the AOD and the column backscatter coefficient is 0.76
198 (Fig 2c). Four tests were designed to investigate the impacts of aerosols and
199 urbanization on typical haze events. Test 1: Both urban and aerosol impacts were
200 considered in the simulation. We updated the grid AOD distribution hourly as the input
201 field for the RRTMG radiation scheme in Domain 2. Test 2: Only aerosol impact was

202 considered in the simulation, and we replaced the urban grids with cropland to shield
203 the impact of urbanization. Test 3: Only urban impact was considered, and the direct
204 radiative forcing of aerosols was not considered in the simulation. Test 4: Both urban
205 and aerosol impacts were not considered in the simulation.

206

207 The model evaluation results for the four tests are shown in Table 2. As the service
208 operational system, the RMAPS-ST model assessment report indicated that the model
209 performance was satisfactory (Fan et al. 2018). We evaluated not only the conventional
210 meteorological variables (including temperature, humidity and wind speed) but also
211 unconventional but important variables for this study (including radiation and surface
212 heat flux). A total of 309 meteorological station data points were used to evaluate the
213 conventional variables. The unconventional variables were evaluated according to the
214 observational data from 140 m of the Beijing meteorological tower. Test 1 was found
215 to be the best simulation and considered both the urban and aerosol impacts. The
216 deficiency of observation sites, interpolation methods and the height differences
217 between the observations and simulations resulted in higher root mean square error
218 (RMSE) values for radiation and heat flux than for the other variables.

219

220 **3 Results**

221 **3.1 Observation and weather condition analysis**

222 A typical continuous severe heavy haze event occurred from the 15th to 22nd of
223 December 2016 in the BTH region. Three stages dominated by three different synoptic
224 patterns controlled the formation of this haze. In the first stage, northwest airflow in
225 front of a ridge of high pressure was observed in the BTH region at a height of 700 to
226 500 hPa and in eastern China at a height of 850 hPa on the 15th to 16th of December,
227 which induced a sharp warming pattern (Fig 3a and b). At the surface, Beijing was
228 located under the front of the high-pressure system to under the southwest airflow in
229 front of the low-pressure system (Fig 4), which favored pollutant transport from Hebei
230 Province to Beijing. From the 17th to the night of the 18th, the control system turned to

231 latitude circulation at 700 to 500 hPa over the BTH region (there was a trough line south
232 of 40°N at 2000 LST on the 17th and 18th) (Fig 3c). There was a northwest wind located
233 north of 40°N and a southwest wind located south of 40°N at 850 hPa (Fig 3d). The
234 near surface was controlled by the northeast airflow located in the inverted low-pressure
235 trough. The weak convergence of the high trough cooperates with the low pressure at
236 the surface, leading to continuous pollution accumulation near the surface. Under this
237 weather situation, the near-surface temperature began to continuously increase from the
238 16th to 18th, and the specific humidity also correspondingly increased (Fig 5a). The near-
239 surface wind speed and pressure decreased during this period (Fig 5b). The
240 concentration of PM_{2.5} gradually increased from the 16th, and the average concentration
241 of PM_{2.5} reached 200 $\mu\text{g}\cdot\text{m}^{-3}$ on the 18th. The density of ozone obviously decreased
242 from the 16th (Fig 5c).

243

244 The MLH significantly declined beginning on the 16th, and the diurnal cycle almost
245 disappeared during this period, which was accompanied by a reduction in visibility with
246 a diurnal variation (Fig 5d). The downward shortwave radiation and the net radiation
247 gradually decreased from the 16th to the 18th, which directly influenced the trend of the
248 variation in ozone (the maximum density of ozone was less than 110 $\text{mg}\cdot\text{m}^{-3}$), while
249 there was little change detected in longwave radiation (Fig 5e). The observed sensible
250 heat flux also decreased from the 16th to the 19th, although the temperature increased,
251 which means that the heat exchange became weaker in the vertical direction, while the
252 latent heat flux changed little (Fig 5f). Southwest airflow was again captured by a wind
253 profiler on the night of the 18th, and the transport layer occurred from 300 to 1500 m,
254 which differs from the previous surface transport pattern (Fig 4).

255

256 In the second stage, an important change occurred on the morning of the 19th of
257 December, when the control system turned to the northwest airflow on the front of the
258 trough over the BTH region at 500 to 850 hPa (Fig 3e and f). After 2000 LST on the
259 19th, obvious warming occurred again at 850 hPa in eastern China (Fig 3h). However,

260 the near-surface maximum temperature and diurnal range in Beijing significantly
261 decreased but with high specific humidity during the 20th to 21st (Fig 5a). According to
262 the surface weather map, the control system turned to the southwest at 1400 LST on the
263 19th, and a large-scale southeast wind appeared in eastern Beijing after 2000 LST, which
264 induced wide advection fog formation overnight (Fig 3g). Due to the influence of the
265 southwest airflow on the trough at 500 hPa, the inverted trough moved east, and Beijing
266 was located in the southeast wind zone. The near-surface pressure increased slightly,
267 and the wind speed remained low at approximately $1 \text{ m}\cdot\text{s}^{-1}$ (Fig 5b). The synoptic
268 system caused the PM_{2.5} concentration to peak (approximately $400 \mu\text{g}\cdot\text{m}^{-3}$ on average
269 and above $500 \mu\text{g}\cdot\text{m}^{-3}$ observed at some stations) and was maintained from the 20th to
270 the 21st in the BTH region. The visibility was less than 400 m, and the diurnal cycle
271 disappeared (Fig 5d). The decrease in the downward shortwave and net radiation during
272 this period was more pronounced than that in the previous three days (Fig 5e). The
273 sensible heat flux also decreased, and the diurnal cycle almost disappeared from the
274 19th to the 20th (Fig 5e). It was not until the strong cold air moved southward in the
275 early morning of the 22nd when the whole atmosphere converted to the northwest stream.
276 The air pollutants were completely removed in the third stage.

277

278

279 ~~The whole atmosphere was converted to the northwest stream only when the strong~~
280 ~~cold air moved southward in the early morning of the 22nd. The air pollutants were~~
281 ~~completely removed in the third stage.~~

282

283 **3.2 Interaction between the impacts of urbanization and aerosols on haze events**

284 Four impacts were analyzed as follows. Urban impact under the aero scenario (UI_aero)
285 was represented by the results of Test 1 minus those of Test 2; urban impact under the
286 no-aero scenario (UI_noaero) was represented by the results of Test 3 minus those of
287 Test 4; the impact of the urbanization scenario was represented by the results of Test 1
288 minus those of Test 3 (AI_urban); the impact without urbanization was represented by

289 the results of Test 2 minus those of Test 4 (AI_nourban). The interaction between
290 urbanization and aerosols on local meteorological and regional transportation was
291 discussed.

292

293 **3.2.1 The impact on the local area**

294 The quantitative results of the interaction between urbanization and aerosols are shown
295 in Table 3. Temperature is one of the most sensitive variables affected by urbanization
296 and aerosols and is also the most concerning variable. The impact of urbanization on
297 the near-surface temperature displays diurnal variation in the Beijing area. The warming
298 effect of urbanization was dominant at night. The urban impact on temperature was
299 partly offset under aerosol conditions when comparing the results of UI_aero and
300 UI_noaero, especially during the daytime (Fig 6a, red lines). The urban impact always
301 showed a positive contribution to the temperature throughout the day under the no-
302 aerosol scenario, while the urban impact became slightly negative during the daytime
303 under the aerosol scenario. The maximum difference between UI_aero and UI_noaero
304 occurred on the 20th and 21st, when the AOD value reached its maximum, and the
305 difference almost disappeared on the 15th and 22nd, with a small AOD (Fig 2b). The
306 results indicate that the impact of urbanization on temperature is reduced by aerosols,
307 which is consistent with the findings of Yang et al. (2020). The average urban impact
308 on temperature in Beijing during the 16th to 19th with a PM_{2.5} concentration of
309 approximately 200 mg·m⁻³ was a reduction of 0.42°C according to UI_aero and a
310 reduction of 0.60°C according to UI_noaero. This result means that aerosols reduce the
311 urban impact on temperature by 30%. When the concentration of PM_{2.5} reached 500
312 mg·m⁻³ from the 20th to the 21st, the aerosols reduced urbanization-related warming by
313 54%.

314

315 The impact of aerosols on temperature is negative and without a diurnal cycle under the
316 urbanization scenario for the whole day (Fig 6a, blue lines). However, the impact of
317 aerosols captured by AI_nourban is significant and displays a diurnal cycle. Another

318 important observation is that the impact of aerosols on temperature under the no-urban
319 scenario is not always negative. There is a slight warming period at dawn in the
320 AI_nourban scenario, which may be because the longwave radiation is increased
321 (Jacobson, 1998; Rudich et al., 2007). The average impact of aerosols on temperature
322 in Beijing was -0.16°C with urbanization and -0.34°C without urbanization from the
323 16th to the 19th. The impact of aerosols was -0.19°C with urbanization and -0.43°C
324 without urbanization from the 20th to the 21st. Urbanization decreased the impact of
325 aerosols by 53% under moderate pollution and by up to 56% under heavy pollution.
326 Two different impacts of aerosols on urban-related warming were observed. There was
327 a reducing effect in the daytime with a strength of approximately 30 to 50% of the
328 concentration, and an increasing effect occurred at dawn with a strength of
329 approximately 28%. Urbanization reduced the aerosol-related cooling effect by
330 approximately 54%.

331

332 The observed specific humidity continued to increase as the aerosol concentration
333 increased (Fig 5b) and was closely related to the UHI effect and aerosol composition
334 (Zhang et al. 2010; Sun et al., 2013; Wang et al., 2020). The specific humidity also
335 increased with urbanization throughout the day (Fig 6b, red lines). Similar to
336 temperature, urbanization had a more pronounced impact on specific humidity at night.
337 The average urban impact on specific humidity was $3.66 \times 10^{-2} \text{ g} \cdot \text{kg}^{-1}$ according to
338 UI_aero and $4.78 \times 10^{-2} \text{ g} \cdot \text{kg}^{-1}$ according to UI_noaero from the 16th to 19th and 3.08×10^{-2}
339 and $4.48 \times 10^{-2} \text{ g} \cdot \text{kg}^{-1}$ from the 20th to 21st. Aerosols not only reduced the urban impact
340 on the average daily specific humidity by 23.43% but also reduced the diurnal range of
341 specific humidity.

342

343 In contrast to urbanization, aerosols were found to reduce the specific humidity (Fig 6b,
344 blue lines). The impact of aerosols under the urbanization scenario was small and did
345 not exhibit a diurnal pattern. However, the impact of aerosols under the no-urban
346 scenario was more distinct and exhibited a diurnal cycle. The average impact of aerosols

347 on specific humidity was $-0.88 \text{ g}\cdot\text{kg}^{-1}$ according to AI_urban and $-1.36 \text{ g}\cdot\text{kg}^{-1}$ according
348 to AI_nourban throughout the study period. Urbanization reduced the impact of
349 aerosols on specific humidity by 35.3%. The impacts of urbanization and aerosols on
350 humidity were slightly greater than those of aerosols on urban impacts.

351

352 There was no effect of urbanization on downward shortwave radiation according to
353 both UI_aero and UI_noaero (Fig 6c, red lines), although the value was not absolutely
354 related to aerosols because of model uncertainty. Aerosols reduce the downward
355 shortwave radiation during the daytime, and the differences between AI_urban and
356 AI_nourban are very small.

357

358 The average decrease in shortwave radiation caused by aerosols was approximately 7%
359 of the total downward shortwave radiation during the 16th to the 20th and up to 17%
360 when the PM_{2.5} was greater than $400 \mu\text{g}\cdot\text{m}^{-3}$. The urban impact increased the longwave
361 radiation at night according to UI_aero, while the impact of urbanization was always
362 positive for longwave radiation during the study period according to UI_noaero (Fig
363 6d, red lines). Because it is closely related to temperature, the urban impact on
364 longwave radiation was also reduced by aerosols, with reductions of 83% from the 16th
365 to the 19th and 97% from the 20th to the 21st. The impact of aerosols on longwave
366 radiation was smaller-less than that of shortwave radiation, and there was a slight
367 decrease captured by AI_urban with an increase from noon on the 20th to nighttime on
368 the 21st. The impact of aerosols decreased the longwave radiation captured by
369 AI_nourban during the 16th to the 20th and increased it on the night of 21st (Fig 6d, blue
370 lines). Urbanization reduced the impact of aerosols on longwave radiation by 67%,
371 while aerosols reduced the urban impact on longwave radiation by 89%. The impacts
372 of urbanization and aerosols on longwave radiation are unimportant because they are
373 both smaller than $2 \text{ W}\cdot\text{m}^{-2}$.

374

375 The change in radiation further alters the MLH. Previous studies suggested that the

376 MLH is important for the diffusion of pollutants and haze formation (Sun et al. 2013;
377 Quan et al. 2014). Previous studies on urbanization indicated that urban-induced
378 warming will increase the MLH during the daytime (Wang et al., 2007; Miao et al.
379 2012), and the results of UI_noaero showed the same pattern. However, when we
380 introduced aerosols into the simulation, urbanization was found to decrease the MLH
381 during the daytime according to UI_aero. The impact of aerosols decreased the average
382 urbanization by 148% during the haze event (Fig 6e, red lines). Aerosols significantly
383 decreased the MLH during the daytime according to both AI_urban and AI_nourban
384 (Fig 6e, blue lines). Urbanization decreased the impact of aerosols on the MLH by 58%
385 during the haze event.

386

387 Urban land use change directly alters the surface heat flux. Urbanization increased the
388 sensible heat flux according to UI_noaero but decreased the sensible heat flux
389 according to UI_aero (Fig 6f, red lines). The impact of aerosols in reducing the urban
390 impact on sensible heat flux was 156% during the haze event. Aerosols reduced the
391 sensible heat flux according to both AI_urban and AI_nourban (Fig 6f, blue lines). The
392 maximum impact of aerosols occurred on the 21st, with the maximum AOD. The impact
393 of urbanization reduced the impact of aerosols on sensible heat flux by 59%.

394

395 There was little effect of urbanization on latent heat flux because the observed latent
396 heat flux in urban areas was small (Fig 6g, red lines, and Fig 5e). Aerosols decreased
397 the latent heat flux, and the impact increased with increasing AOD (Fig 6g, blue lines).
398 The impact of urbanization reduced the impact of aerosols on the latent heat flux by
399 48%.

400

401 The above results indicate that the offsetting effect of aerosols on urbanization is more
402 important than the impact of urbanization on aerosols on local weather.

403

404 **3.2.2 Effects on regional circulation**

405 There are few valuable findings from the diurnal average wind speed analysis because
406 the average wind speed was low during the haze event. Wind speed is likely to become
407 more meaningful during the spatial analysis of wind vectors. There are two main
408 transmission processes of pollution from Hebei Province to Beijing during this haze
409 process according to the weather map and wind profile analysis (Fig 4). Accordingly,
410 the diurnal pattern of PM_{2.5} in Beijing (Fig 5c) also displays two increasing processes
411 on the 16th and 19th (from 1800 to 2400 LST). The observed near-surface wind vector
412 displays these two pollutant transport processes (Fig 7). In the first processes, obvious
413 aerosol transport began on the night of the 15th and continued to the night of the 16th
414 (Fig 6). The southwest wind dominated most of the southern part of Hebei Province.
415 The transmission flux was strong during the daytime on the 16th, leading to the
416 concentration of PM_{2.5} continuing to increase in Beijing and in its transmission path.
417 The wind speed remained low from the 17th to the 18th in most of the plain area, and the
418 concentration of PM_{2.5} continued to increase in the southwest and northeast of Hebei
419 Province. The second processes began at 1400 LST on the 19th, and the south wind
420 dominated the south of Beijing and turned to the southwest in Beijing at 1400 to 1800
421 LST. The dominant wind direction turned to the southwest at 2200 LST in the southern
422 part of Hebei Province with a rapid increase in the concentration of PM_{2.5}.

423

424 Most industrial aerosols in Beijing are transported from the southwest and northeast of
425 Hebei Province due to the control of pollutant discharge in the Beijing area during haze
426 events. Therefore, the impact of urban areas and aerosols on transport, namely, wind
427 fields, is very important for air quality in Beijing. The modeling results show that
428 urbanization not only increased the temperature in urban areas (Fig 8a and b) but also
429 increased the average south-wind transport flux in the two main transmission processes
430 of pollution in the southwest area of Beijing (Fig 8a and b). The transmission flux
431 captured by UI_noaero was stronger than that captured by UI_aero. The local cyclonic
432 circulation induced by urbanization further induced upward movement, which was
433 beneficial to diffusion conditions. Although aerosols decrease the transmission flux

434 induced by urbanization, the strength of local cyclonic circulation is also reduced by
435 aerosols. Furthermore, the aerosols reduced the temperature in most of the plain area in
436 Hebei Province (Fig 8c and d). Urbanization decreased the impact of aerosols on
437 temperature. There was no local or systemic effect on the wind field captured by either
438 AI_urban or AI_nourban.

439

440 Taylor diagrams were used to analyze the relative contributions of urbanization and
441 aerosols over time (Fig 9). The daily mean differences in these four types of impact
442 (UI_aero, UI_noaero, AI_urban, and AI_nourban) over the eight days in the Beijing
443 area are shown by Taylor diagrams. UI_noaero shows that temperature continued to
444 increase from Day 1 to Day 5 and reached a maximum on Day 7. The variation in
445 temperature according to UI_aero was small. This result means that the effect of
446 urbanization on temperature is decreased by aerosols. Temperature increased from Day
447 1 to Day 7 according to AI_urban, while AI_nourban showed an increase from Day 3
448 to Day 7. The reduction in the urban impact on temperature by aerosols was more
449 important than the reduction in aerosol impact on temperature by urbanization (Fig 9a).
450 The effect of aerosols on the urban impacts on temperature was more important than
451 the urban impacts on the effects of aerosols on temperature (Fig 9a).

452

453 Specific humidity continued to increase from Day 1 to Day 5 according to UI_noaero,
454 while the variation in specific humidity was small according to UI_aero (Fig 9b).
455 Similar to what was observed for temperature, reducing the urban impact on specific
456 humidity by aerosols is more important than reducing the impacts to aerosols by urban
457 areas. The ventilation coefficient (VC) in UI_aero showed little change over these eight
458 days, and this coefficient showed increases on Days 2, 3, 5, and 6 and decreases on
459 Days 4, 7, and 8 according to UI_noaero. The reduction in the urban impact on the VC
460 by aerosols was more important than the reduction in the impact of aerosols by
461 urbanization. The analysis of shortwave radiation also provided the same conclusion
462 that the reduction in the urban impact on the daily mean by aerosols was more important

463 than the reduction in the impact of aerosols by urbanization (Fig 9d).

464

465 **3.2.3 Impacts on the vertical distribution**

466 In the period from 0000 LST to 0800 LST on the 16th to 20th, there was an interesting
467 phenomenon that temperature was slightly larger in UI_aero than in UI_noaero, and the
468 urban impact reached a maximum at the same time. Such an outcome is easy to overlook
469 if the analysis focuses on only the daily average. Therefore, a detailed vertical
470 temperature and wind field analysis of the four addressed scenarios (UI_aero,
471 UI_noaero, AI_urban, and AI_nourban) was used to determine the mechanism behind
472 this finding (Fig 10).

473

474 The impact on warming by urbanization reached 350 m in UI_aero and 450 m in
475 UI_noaero (Fig 10a and b). Aerosols not only increased the warming impact induced
476 by urbanization but also reduced the warming height. Aerosols increase the near-surface
477 warming effect induced by urbanization because of the absorption of longwave
478 radiation. Although absorption by aerosols was always observed during the study period,
479 the impact increased with the increase in longwave radiation induced by urbanization.
480 Therefore, the warming effect of aerosols may dominate at night in the near-surface
481 layer. This effect further induces urban-related warming to increase and compress this
482 effect to a lower height with a lower MLH in UI_aero than in UI_noaero (Fig 10a). The
483 aerosols reduced the temperature below 450 m in the urban area of Beijing (Fig 10c and
484 d), and the cooling effect was reduced by urbanization below 450 m. Urbanization also
485 reduced the near-surface west wind induced by aerosols in urban areas because of the
486 drag caused by buildings.

487

488 **4 Conclusion**

489 A typical persistent haze process occurred on the 15th to 22nd of December 2016 in the
490 BTH region. The average concentration of PM_{2.5} was approximately 200 $\mu\text{g}\cdot\text{m}^{-3}$, and
491 the maximum was 695 $\mu\text{g}\cdot\text{m}^{-3}$. The interaction between aerosols and urbanization on

492 haze events was investigated in this study. Four tests were designed using RMAPS-ST
493 to study the mechanism of the impacts of aerosols and urbanization.

494

495 Two different impacts of aerosols on urban-related warming were found. A reducing
496 effect occurred during the daytime, and the strength was approximately 30 to 50% of
497 the concentration. An increasing effect occurred at dawn, and the strength was
498 approximately 28%, which is important for haze formation. The combined effect was a
499 reducing effect on the daily mean of urban-related warming. Urbanization reduced the
500 aerosol-related cooling effect by approximately 54% during the haze event, and the
501 strength of the impact changed little with increasing aerosol content. The impact of
502 urbanization on the effect of aerosols on humidity is slightly larger than the impact of
503 aerosols on urban impact. Aerosols reduce the average downward shortwave radiation
504 from 7% to 17% with concentrations of $PM_{2.5}$ of 200 to 400 $\mu g \cdot m^{-3}$. There is no urban
505 impact on downward shortwave radiation or an impact of aerosols on shortwave
506 radiation. The impacts of urban areas and aerosols on longwave radiation are both
507 smaller than $2 W \cdot m^{-2}$. The most significant impact of aerosols is observed on the MLH
508 and sensible heat flux. The decrease in urban impact caused by aerosols reaches 148%
509 for MLH and 156% for sensible heat flux. These values are much larger than those for
510 urbanization, which reduces the impact of aerosols on the MLH and sensible heat flux.
511 There is little urban impact on latent heat flux. However, aerosols decreased the latent
512 heat flux, and the impact was reduced by 48.8% by urbanization. In general, the impact
513 of aerosols on urban impact is more important than the impact of urbanization on
514 aerosol impacts in terms of regional averages.

515

516 Urbanization increased the wind speed southwest of the Beijing area and the local
517 cyclonic circulation in the urban area of Beijing during the two main transmission
518 processes. Although aerosols reduced the urban-related southwest transmission, they
519 worsened the diffusion conditions in urban areas. The impact of urbanization on wind
520 fields, namely, the transport of pollutants, is more important than that of aerosols.

521 However, the interaction between urbanization and aerosols may enhance the
522 accumulation of pollution and weigh against diffusion.

523

524 The impact of aerosols on urban-related warming is more significant than the impact of
525 urbanization on aerosol-related cooling according to spatial statistical analysis. Similar
526 results were found for absolute humidity, VC and shortwave radiation. Aerosol-related
527 warming is dominant at dawn in the near-surface layer. Aerosols increase urban-related
528 warming and reduce the impact height of urban-related warming. This further enhances
529 stability and reduces the MLH.

530 **5 Discussion**

531 In this study, it was easier to distinguish the impacts of aerosols and urbanization by
532 using RMAPS-ST with AOD hourly inputs than with RMAPS-Chem. One reason for
533 this difference is that the model performance of RMAPS-ST is much better than that of
534 RMAPS-Chem in meteorological fields. Although real-time feedback in modeling is
535 not provided, RMAPS-ST is more efficient and more suitable for short-term operational
536 forecasting.

537

538 This study not only qualified the impacts of aerosols and urbanization on haze events
539 but also analyzed the interaction between aerosols and urbanization during haze events.
540 This research will help to improve air quality under the continuous
541 urbanization and sustainable development of large cities.

542

543 The government has taken a series of emission reduction measures, including limiting
544 industrial emissions and vehicle plate number traffic restriction measures, to improve
545 the air quality in the BTH region. The policies have been effective in reducing aerosols.
546 At the same time, urbanization continues mainly in the areas around Beijing (such as
547 the Xiongan New Area). The results of this study show that the combined impact of
548 urbanization and decreasing aerosols will increase the downward shortwave radiation
549 and further increase the surface temperature and ozone concentration in the boundary

550 layer. Previous studies indicated that ozone generally increases with temperature and
551 decreases with humidity (Camalier et al., 2007; Cardelino et al., 1990). It is well known
552 that ozone is not only a pollutant but also a greenhouse gas. Therefore, ozone will form
553 a positive feedback mechanism to induce warming and ozone pollution in the boundary
554 layer. This feedback will pose a new challenge regarding how to reduce ozone pollution
555 in urban areas. Some studies have suggested that urban greening can effectively reduce
556 ozone pollution (Nowak et al., 2000; Benjamin and Winer, 1998). More attempts should
557 be made to add the interaction between urbanization and ozone in regional models.

558

559 **Acknowledgments**

560 This work was supported by the Beijing National Science Foundation of China
561 (Grant No. 8171002), the National Natural Science Foundation (41705088) and
562 the National Key R&D Program of China (2019YFA0607202).

563

564 **Data availability**

565 The data in this study are available from the corresponding author upon request
566 (tqq@dq.cern.ac.cn).

567

568 **Author contribution**

569 Miao Yu designed the research and wrote the paper. Guiqian Tang conducted the
570 measurements and reviewed the paper. Yang Yang conducted modeling tests. Qingchun
571 Li and Yonghong Wang performed synoptic analysis. Shiguang Miao, Yizhou Zhang
572 and Yusi Wang reviewed and commented on the paper.

573

574 **Competing interests**

575 The authors declare that they have no conflicts of interest to disclose.

576

577 **Table 1 RMAPS-ST model settings.**

WRF v3.8.1	D01	D02
------------	-----	-----

Horizontal grid	649×400	550×424
Grid horizontal spacing (km)	9	3
Vertical layers	49	
PBL	YSU (Hong et al., 2006)	
Microphysics	Thompson (Thompson et al., 2008)	
Cumulus	Kain-Fritsch (Kain, 2004)	None
LW radiation	RRTMG	
SW radiation	RRTMG	
LSM	Noah LSM+SLUCM	
Urban parameter values	Modified according to Miao and Chen (2014)	

578

579

580

581

582

583

Table 2 Model evaluation (RMSE and BIAS) for the four tests.

	Test 1		Test 2		Test 3		Test 4	
	RMSE	BIAS	RMSE	BIAS	RMSE	BIAS	RMSE	BIAS
Temperature	1.27	0.35	1.45	-0.73	2.12	1.04	1.78	-0.45
Specific	0.26	-	0.31	0.019	0.34	-0.05	0.29	0.03
Wind speed	1.62	0.97	2.08	1.68	1.85	1.04	1.96	1.67
Shortwave	40.91	11.85	40.95	11.89	47.35	17.45	46.26	16.45
Longwave	51.39	-	51.32	-	51.24	-	52.76	44.97
Sensible heat	8.09	-1.19	9.13	-3.92	9.34	-3.43	12.3	-6.17
Latent heat	14.09	-5.75	14.52	-5.95	14.85	-5.87	16.76	-6.23

584

585

586

587

588

589

Table 3 Quantitative results of the interaction between urbanization and aerosols

	Temperature		Specific humidity		Longwave		MLH	Sensible heat flux W·m ⁻²	Latent heat flux W·m ⁻²
	°C		×10 ⁻² g kg ⁻¹		W·m ⁻²				
Time	16 th -19 th	20 th -21 st	16 th -19 th	20 th -21 st	16 th -19 th	20 th -21 st	16 th -21 st	16 th -21 st	16 th -21 st

UI_aero	0.42	0.19	3.66	3.08	0.10	-0.02	-1.97	-1.01	0.03
UI_noaero	0.60	0.35	4.78	4.48	0.62	0.51	4.04	1.74	0.49
AI_urban	-0.16	-0.19		-0.88		-0.24		-4.37	-1.64
AI_nourban	-0.34	-0.43		1.36		-0.73		-10.38	-4.02

590

591

592 References

593 Benjamin, M. T., Winer, A. M.: Estimating the ozone-forming potential of urban trees and shrubs,
594 Atmospheric Environment, 32(1), 53-68, 1998.

595 Camalier, L., Cox, W. , and Dolwick, P.: The effects of meteorology on ozone in urban areas and
596 their use in assessing ozone trends, Atmospheric Environment, 41(33), 7127-7137, 2007.

597 Cao, C., Lee, X., Liu, S., Schultz, N., Xiao, W., Zhang, M., and Zhao, L.: Urban heat islands in
598 China enhanced by haze pollution, Nature Communications, 7(1), 1-7, 2016.

599 Cardelino, C. A., and Chameides, W. L.: Natural hydrocarbons, urbanization, and urban
600 ozone, Journal of Geophysical Research, 95(D9), 13971, 1990.

601 Chen, H., and H. Wang: Haze Days in North China and the associated atmospheric circulations
602 based on daily visibility data from 1960 to 2012, J. Geophys. Res. Atmos., 120, 5895–5909,
603 2015.

604 Coulter, R.L.: A Comparison of three methods for measuring mixing-layer height, J Appl
605 Meteor, 18(11):1495-1499, 1979.

606 Crutzen, P. J.: New directions: the growing urban heat and pollution ‘island’ effect-impact on
607 chemistry and climate, Atmos. Environ, 38, 3539–3540, 2004.

608 Fan, S.: Assessment report of regional high resolution model (RMAPS-ST), IUM Technical Note
609 IUM/2018-1, Beijing, China: IUM, 2018.

610 Folberth, G. A., Rumbold, S. T., Collins, W. J., and Butler, T. M.: Global radiative forcing and
611 megacities, Urban Climate., 1, 4–19, 2014.

612 Grimm, N. B. et al.: Global change and the ecology of cities, Science, 319 (5864), 756–760, 2008.

613 Grimm, C.S. B., Kuttler, W., Lindqvist, S., and Roth, M.: Urban climatology icuc6, International
614 Journal of Climatology, 27(14), 1847-1848, 2010.

615 Grimm, S.U. E.: Urbanization and global environmental change: local effects of urban warming,
616 Geographical Journal, 173(1), 83-88, 2007.

617 Guo, J., Miao, Y., Zhang, Y., Liu, H., Li, Z., Zhang, W., ...and Zhai, P.: The climatology of planetary
618 boundary layer height in China derived from radiosonde and reanalysis data, Atmospheric
619 Chemistry and Physics, 16(20), 13309-13319, 2016.

620 Huang, J., Minnis, P., Yi, Y., Tang, Q., Wang, X., Hu, Y., ... and Winker, D. M.: Summer dust aerosols
621 detected from CALIPSO over the Tibetan Plateau, Geophysical Research Letters, 34(18),
622 DOI:10.1029/2007GL029938, 2007.

623 Huang, J., Minnis, P., Chen, B., Huang, Z., Liu, Z., Zhao, Q., ... and Ayers, J. K.: Long-range
624 transport and vertical structure of Asian dust from CALIPSO and surface measurements during
625 PACDEX, Journal of Geophysical Research, 113, DOI:10.1029/2008JD010620., 2008a.

626 Huang J., W. Zhang, J. Zuo, J. Bi, J. Shi, X. Wang, Z. Chang, Z. Huang, S. Yang, B. Zhang, G. Wang,
627 G. Feng, J. Yuan, L. Zhang, H. Zuo, S. Wang, C. Fu and J. Chou.: An overview of the semi-arid
628 climate and environment research observatory over the Loess Plateau, Advances in Atmospheric
629 Sciences, 25(6), 1-16. DOI: 10.1007/s00376-008-0906-7, 2008b.

630 Hong, S. Y., Noh, Y., and Dudhia, J.: A new vertical diffusion package with an explicit treatment of
631 entrainment processes, Monthly Weather Review, 134, 2318–2341, 2006.

632 Jacobson, M. Z.: Studying the effects of aerosols on vertical photolysis rate coefficient and
633 temperature profiles over an urban airshed, Journal of Geophysical Research, 103, 10593–10604,

634 1998.

635 Kain, J. S.: The Kain–Fritsch convective parameterization: An update, *Journal of Applied*
636 *Meteorology*, 43, 170–181, 2004.

637 Li, D. and Bou-Zeid, E.: Synergistic interaction between urban heat islands and heat waves: the
638 impact in cities is larger than the sum of its parts, *J. Appl. Meteorol. Climatol*, 52, 2051–2064,
639 2013.

640 Liu, Q., Geng, H., Chen Y.: Vertical distribution of aerosols during different intense dry haze period
641 around Shanghai, *China Environmental Science* (in Chinese), 32(2), 207-213, 2012.

642 Miao, S, Dou J., Chen, F., Li, J., and Li A.: Analysis of observations on the urban surface energy
643 balance in Beijing, *Science China Earth Sciences*, 055(11), 1881-1890, 2012.

644 Miao, S. and Chen, F.: Enhanced modeling of latent heat flux from urban surfaces in the
645 Noah/single-layer urban canopy coupled model, *Science China Earth Sciences*, 057(10), 2408-
646 2416, 2014.

647 Miao, S., Chen, F., Li, Q., and Fan, S.: Impacts of urban processes and urbanization on summer
648 precipitation: A case study of heavy rainfall in Beijing on 1 August 2006, *Journal of Applied*
649 *Meteorology and Climatology*, 50, 806–825, <https://doi.org/10.1175/2010JAMC2513.1>, 2011

650 Miao, Y., Guo, J., Liu, S., Liu, H., Li, Z., Zhang, W., and Zhai, P.: Classification of summertime
651 synoptic patterns in Beijing and their associations with boundary layer structure affecting aerosol
652 pollution., *Atmos. Chem. Phys*, 17(4), 3097-3110, 2017.

653 Nowak, D. J., Civerolo, K. L., Rao, S. T., Sistla, G., Luley, C. J., and Crane, D. E.: A modeling study
654 of the impact of urban trees on ozone, *Atmospheric Environment*, 34(10), 1601-1613, 2000.

655 Oke, T.R.: The energetic basis of the urban heat island, *Quarterly Journal of the Royal*
656 *Meteorological Society*, 108, 1–24, 1982.

657 Oke, T.R.: The heat island of the urban boundary layer: Characteristics, causes and effects, *Wind*
658 *Climate in Cities*, 81-107, 1995.

659 Pei, L., Yan, Z., Chen, D., & Miao, S.: Climate variability or anthropogenic emissions: which caused
660 Beijing Haze? *Environmental Research Letters*, 15(3), 034004, 2020.

661 Quan, J., Tie, X., Zhang, Q., Liu, Q., Li, X., and Gao, Y., et al.: Characteristics of heavy aerosol
662 pollution during the 2012–2013 winter in Beijing, China, *Atmospheric Environment*,
663 88(Complete), 83-89, 2014.

664 Ren, Y., Zhang, H., Wei, W., Wu, B., Cai, X., and Song, Y.: Effects of turbulence structure and
665 urbanization on the heavy haze pollution episodes, *Atmospheric Chemistry and Physics*, 19.
666 1041-1057, 2019.

667 Rudich, Y., Donahue, N. M. & Mentel, T. F. Aging of organic aerosol: bridging the gap between
668 laboratory and field studies, *Ann. Rev. Phys. Chem.*, 58,321–352, 2007.

669 Ruiz-Arias, J. A., Dudhia, J., & Gueymard, C. A.: A simple parameterization of the short-wave
670 aerosol optical properties for surface direct and diffuse irradiances assessment in a numerical
671 weather model. *Geoscientific Model Development*, 7(3), 1159-1174, 2014.

672 Skamarock, W. C., Klemp, J. B., Dudhia, J., Gill, D. O., Barker, D., Wang, W., and Powers, J. G.: A description of
673 the advanced research WRF version 3, NCAR/TN-475 + STR, 2008.

674 Sun, Y., Wang, Z., Fu, P., Jiang, Q., Yang, T., Li, J., and Ge, X.: The impact of relative humidity on
675 aerosol composition and evolution processes during wintertime in Beijing, China, *Atmospheric*
676 *Environment*, 77, 927-934, 2013.

677 Taha, H.: Urban climates and heat islands: albedo, evapotranspiration, and anthropogenic heat,
678 Energy and Buildings, 25, 99–103, 1997.

679 Tang, G., Zhu, X., Hu, B., Xin, J., and Wang, Y.: Impact of emission controls on air quality in Beijing
680 during APEC 2014: lidar ceilometer observations, Atmospheric Chemistry and Physics, 15(21),
681 12667-12680, 2015.

682 Tang, G. , Zhang, J. , Zhu, X. , Song, T. , and Wang, Y. : Mixing layer height and its implications
683 for air pollution over Beijing, China, Atmospheric Chemistry and Physics, 16(4), 2459–2475,
684 2016.

685 Tao, W., Liu, J., Ban-Weiss, G. A., Hagnlustaine, D. A., Zhang, L., Zhang, Q.,... and Tao, S.: Effects
686 of urban land expansion on the regional meteorology and air quality of eastern China,
687 Atmospheric Chemistry and Physics, 15(15), 8597–8614, <https://doi.org/10.5194/acp-15-8597-2015>, 2015.

688 Thompson, G., Field, P. R., Rasmussen, R. M., & Hall, W. D.: Explicit forecasts of winter
689 precipitation using an improved bulk microphysics scheme. Part II: Implementation of a new
690 snow parameterization, Monthly Weather Review, 136, 5095–5115, 2008.

691 Wang, K., Wang, J., Wang, P., Sparrow, M., Yang, J., Chen, H.: Influences of urbanization on
692 surface characteristics as derived from the Moderate-Resolution Imaging Spectroradiometer:
693 A case study for the Beijing metropolitan area, Journal of Geophysical Research, 112 (D22),
694 doi:10.1029/2006jd007997, 2007.

695 Wang, Y., Yu, M., Wang, Y., Tang, G., Song, T., Zhou, P., ... and Zhu, X.: Rapid formation of intense
696 haze episodes via aerosol–boundary layer feedback in Beijing, Atmospheric Chemistry and
697 Physics, 20(1), 45-53, 2020.

698 Wei, W., Zhang, H., Wu, B., Huang, Y., Cai, X., Song, Y., and Li, J.: Intermittent turbulence
699 contributes to vertical dispersion of PM_{2.5} in the North China Plain: cases from Tianjin,
700 Atmospheric Chemistry and Physics, 18, 12953–12967, <https://doi.org/10.5194/acp-18-12953-2018>, 2018.

701 Wu, D., Wu, X., Li, F., et al.: Temporal and spatial variation of haze during 1951-2005 in Chinese
702 mainland, Acta Meteorologica Sinica (in Chinese), 68(5), 680-688, 2010.

703 Xu, X., Chen, F., Barlage, M., Gochis, D., Miao, S., and Shen, S.: Lessons learned from modeling
704 irrigation from field to regional scales, Journal of Advances in Modeling Earth Systems, 11,
705 2428–2448, <https://doi.org/10.1029/2018MS001595>, 2019.

706 Yang, Y., Zheng, Z., Yim, S. Y. L., Roth, M., Ren, G., Gao, Z., et al.: PM_{2.5} pollution modulates
707 wintertime urban heat island intensity in the Beijing - Tianjin - Hebei Megalopolis, China,
708 Geophysical Research Letters, 47, e2019GL084288. <https://doi.org/10.1029/2019GL084288>,
709 2020.

710 Yu, M., and Y. Liu: The possible impact of urbanization on a heavy rainfall event in Beijing,
711 Journal of Geophysical Research: Atmospheres , 120, 8132–8143, doi:10.1002/2015JD023336,
712 2015.

713 Yu, M., Miao, S., and Li, Q.: Synoptic analysis and urban signatures of a heavy rainfall on 7 August
714 2015 in Beijing, Journal of Geophysical Research: Atmospheres, 122, 65–78,
715 <https://doi.org/10.1002/2016JD025420>, 2017.

716 Yu, M., Y. M. Liu, Y. F. Dai, et al.: Impact of urbanization on boundary layer structure in Beijing,
717 Climatic Change, 120(1-2), 123-136, 2013.

720 Zhai, S.X, Jacob, Daniel, Wang, X., Lu, S., Li, K. , Zhang, Y.Z., Gui, K., Zhao, T.L., and Liao, H.: Fine particulate matter (PM2.5) trends in China, 2013–2018: contributions from meteorology, Atmospheric Chemistry and Physics, 19(16), 11031-11041, 2019.

721

722

723 Zhang, C., Liu, C., Hu, Q., Cai, Z., Su, W., Xia, C., ... and Liu, J.: Satellite UV-Vis spectroscopy: implications for air quality trends and their driving forces in China during 2005–2017, Light- Science & Applications, 8(1), 1-12, 2019.

724

725 Zhang, N., Gao, Z., Wang, X., and Chen, Y.: Modeling the impact of urbanization on the local and regional climate in Yangtze River Delta, China, Theoretical and applied climatology, 102(3-4), 331-342, 2010.

726

727

728 Zhang, W., Zhuang, G., Guo, J., Xu, D., Wang, W., and Baumgardner, D.,... and Yang, W.: Sources of aerosol as determined from elemental composition and size distributions in Beijing, Atmospheric Research, 95(2-3), 0-209, 2010.

729

730

731 Zhang, Z., Zhao, X., Xiong, Y., Ma, X.H.: The Fog/Haze Medium-range Forecast Experiments Based on Dynamic Statistic Method, Journal of Applied Meteorological Science (in Chinese), 29(1),57-69, 2018.

732

733

734 Zhao, P., Xu, X., Meng, W. Dong, ... and Zhang, X.L.: Characteristics of haze days in the region of Beijing, Tianjin, and Hebei, China Environmental Science (in Chinese), 31(1), 31-36, 2012.

735

736 Zhao, X., Li, Z., and Xu, J.: Beijing regional environmental meteorology prediction system and its performance test of PM2.5 concentration, Journal of Applied Meteorological Science (in Chinese), 27(2),160-172, 2016.

737

738

739 Zhao, X.J., Li, Z.M., Xu, J.: Modification and performance tests of visibility parameterizations for haze days. Environmental. Science, 40 (4), 1688–1696 (in Chinese), 2019.

740

741 Zhong, S., Qian, Y., Sarangi, C., Zhao, C., Leung, R., Wang, H.,... and Yang, B.: Urbanization effect on winter haze in the Yangtze River Delta region of China, Geophysical Research Letters, 45, 6710–6718, <https://doi.org/10.1029/2018GL077239>, 2018.

742

743

744 Zhong, S., Qian, Y., Zhao, C., Leung, R., and Yang, X. Q.: A case study of urbanization impact on summer precipitation in the Greater Beijing Metropolitan Area: Urban heat island versus aerosol effects, Journal of Geophysical Research: Atmospheres, 120, 10,903–10,914. <https://doi.org/10.1002/2015JD023753>, 2015.

745

746

747

748 Zhong, S., Qian, Y., Zhao, C., Leung, R., Wang, H. L., Yang, B., ... and Liu, D.: Urbanization-induced urban heat island and aerosol effects on climate extremes in the Yangtze River Delta region of China. Atmospheric Chemistry and Physics, 17(8), 5439–5457, <https://doi.org/10.5194/acp-17-5439-2017/>, 2017.

749

750

751

752 Zhu, X., Tang, G., Guo, J., Hu, B., Song, T., Wang, L., Xin, J., Gao, W., Münkel, C., Schäfer, K., Li, X., and Wang, Y.: Mixing layer height on the North China Plain and meteorological evidence of serious air pollution in southern Hebei, Atmospheric Chemistry and Physics, 18, 4897–4910, <https://doi.org/10.5194/acp-18-4897-2018>, 2018.

753

754

755

756

757

758

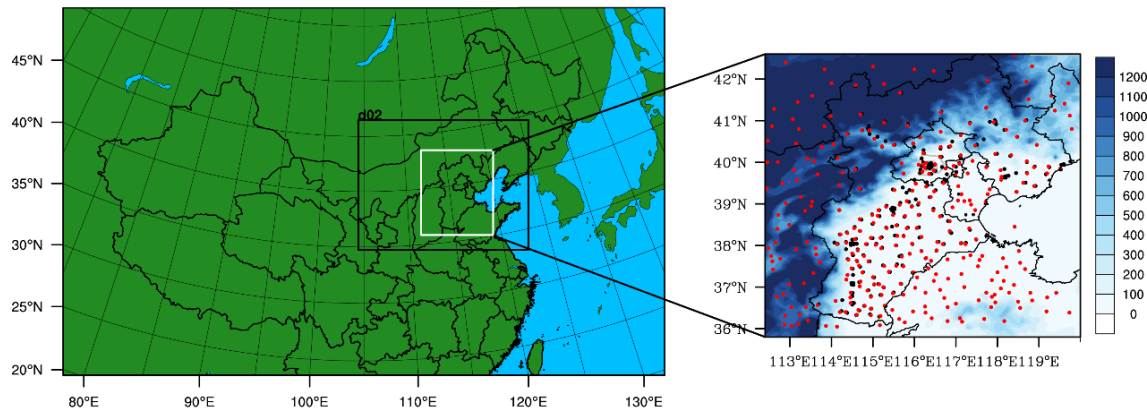
759

760

761

762

763 **Figure**



764

765 Figure 1 Domain configuration of RMAPS-ST and the location of the study area, indicated by the
766 solid white line. The black dots indicate the locations of the 251 environmental monitoring stations,
767 and the red dots represent the 309 meteorological stations in the BTH region, where the gray loop
768 lines show the locations of the second to sixth ring roads. The shading is the terrain height (unit: m).

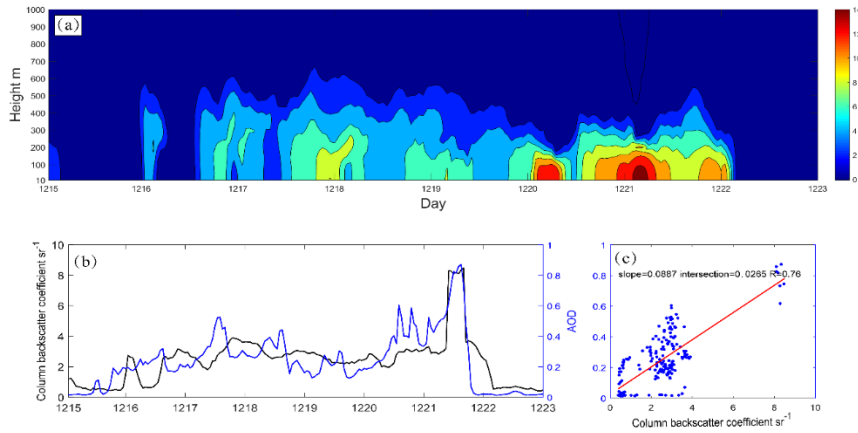
769

770

771

772

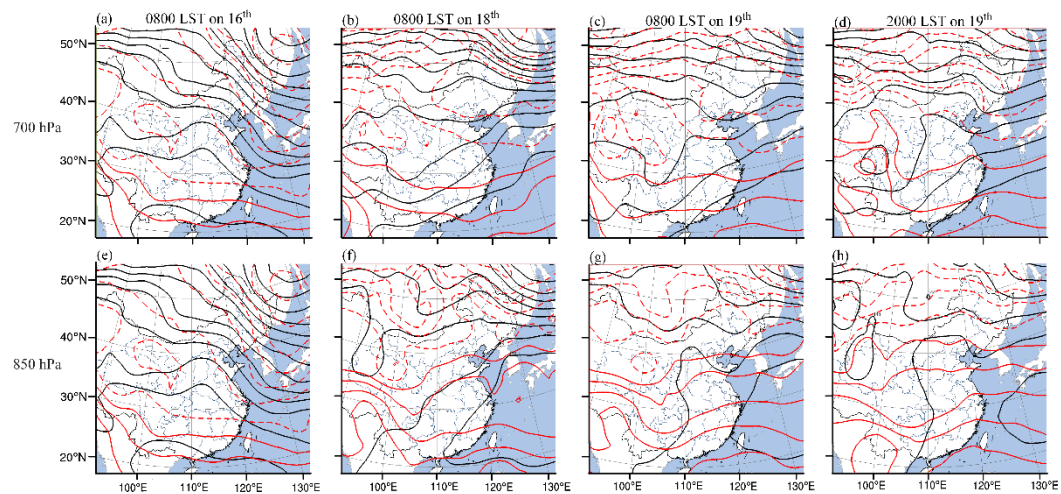
773



774

775 Figure 2 (a) Hourly backscattering coefficient (shading; $\text{Mm}\cdot\text{sr}^{-1}$) observed by single-lens
 776 ceilometers (39.97°N , 116.37°E) from the 15th to 23rd of December; (b) hourly column backscatter
 777 coefficient (black line; sr^{-1}) and AOD used in modeling for Beijing (blue line) and (c) scatter
 778 diagram of hourly column backscatter coefficient and AOD (blue dots) and their correlations (red
 779 line).
 780

781



782

783 Figure 3 Weather maps. (a) 0800 LST on the 16th at 700 hPa; (b) 0800 LST on the 18th at 700 hPa;
 784 (c) 0800 LST on the 19th at 700 hPa; (d) 2000 LST on the 19th at 700 hPa; (e) 0800 LST on the
 785 16th at 850 hPa; (f) 800 LST on the 18th at 850 hPa; (g) 0800 LST on the 19th at 850 hPa; (h) 2000
 786 LST on the 19th at 850 hPa.

787

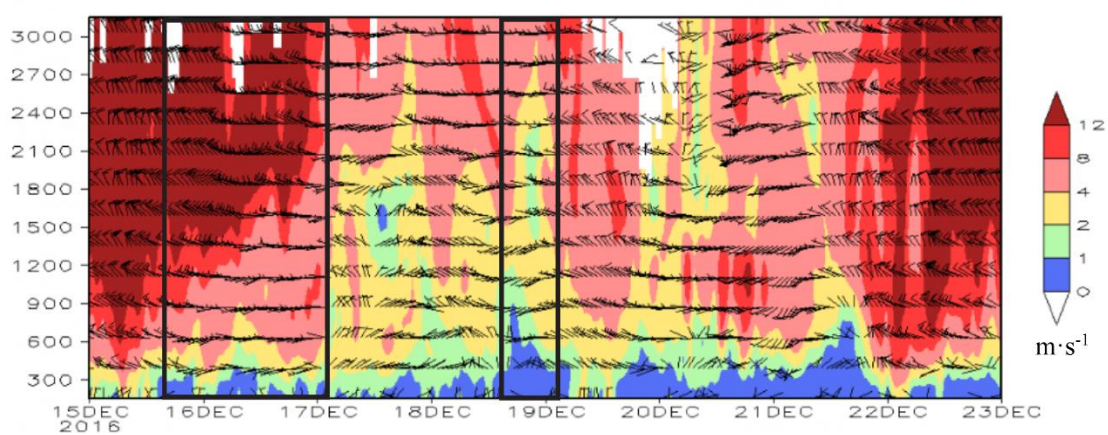
788

789

790

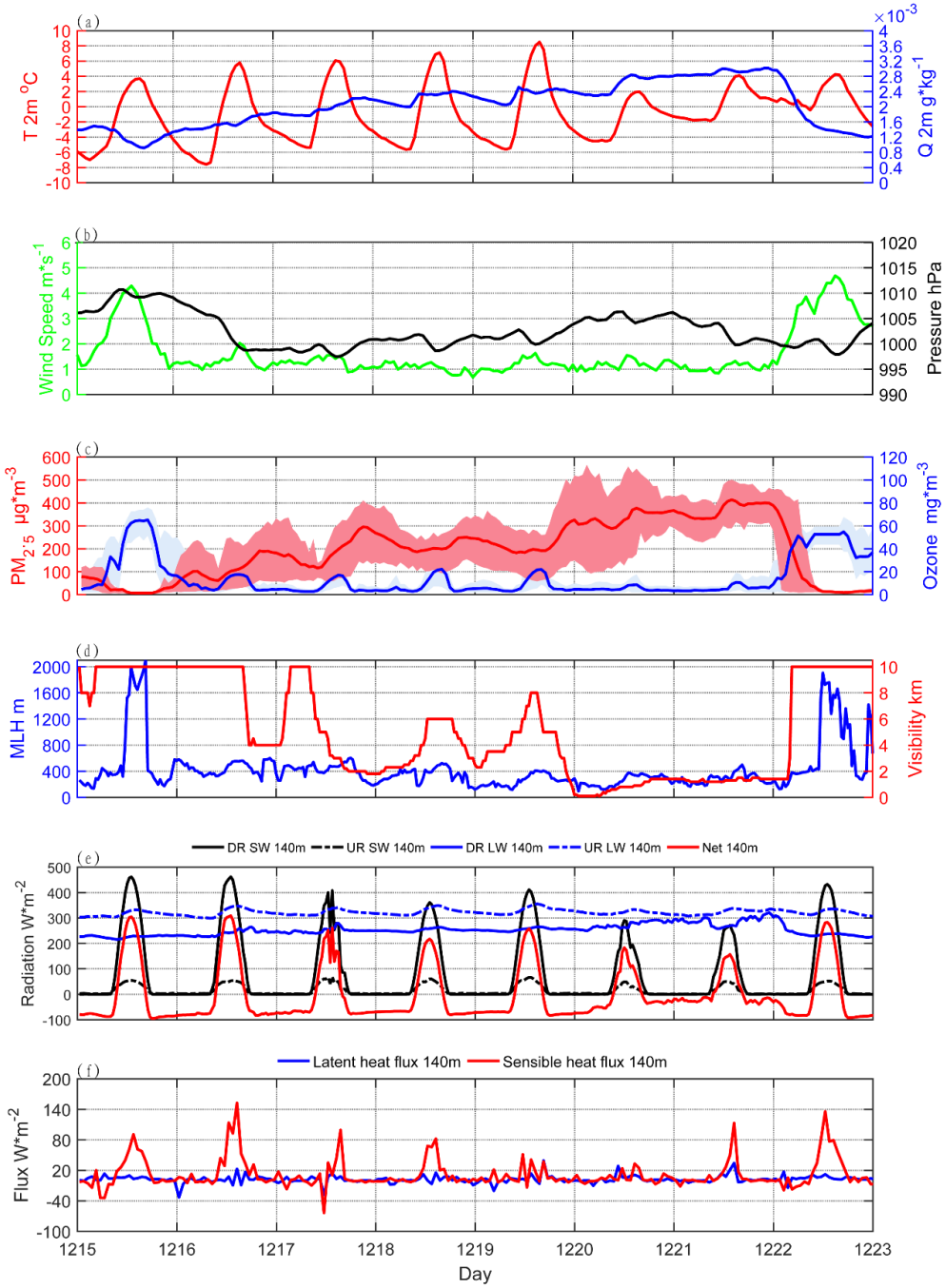
791

792



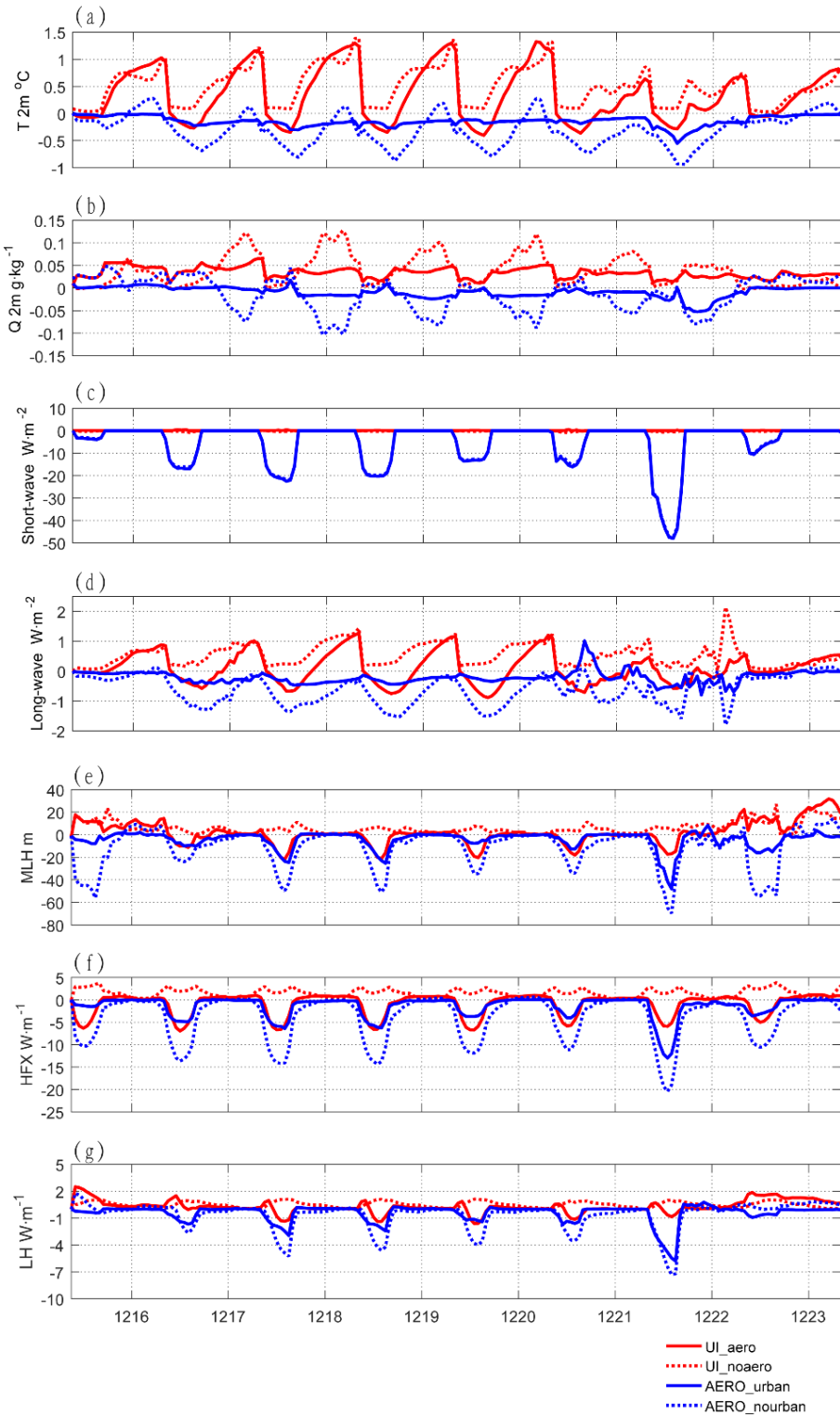
793

794 Figure 4 Hourly wind profile from the 15th to 23rd of December. Wind speed (shading; $\text{m}\cdot\text{s}^{-1}$) and
 795 horizontal wind field (vector; $\text{m}\cdot\text{s}^{-1}$). The black boxes show the two periods of south wind
 796 conveyance.



797

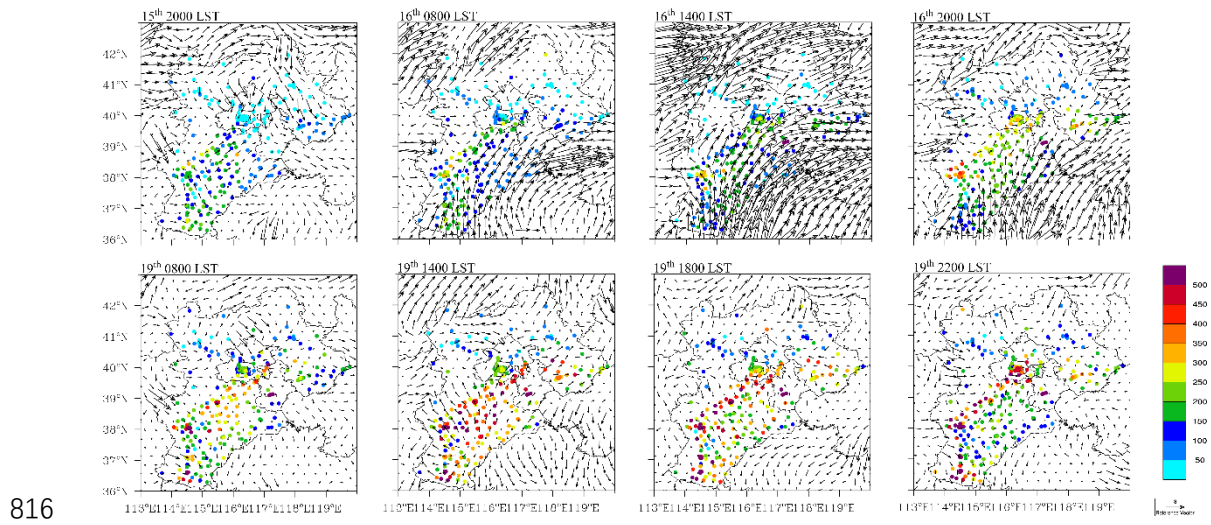
798 Figure 5 Diurnal pattern of observed variables from the 15th to 23rd of December in Beijing. (a)
799 Temperature (red line; $^{\circ}\text{C}$) and absolute humidity (blue line; g kg^{-1}) at 2 m; (b) wind speed at 10
800 m (green line; m s^{-1}) and pressure (black line; hPa); (c) average $\text{PM}_{2.5}$ concentration (red line is
801 the average and the shading indicates the standard deviation; ug m^{-3}) and ozone concentration
802 (blue lines and the shading indicate the standard deviation; mg m^{-3}) of 35 environmental
803 monitoring stations in Beijing; (d) mixing layer height (blue line; m) and visibility (red line; km);
804 (e) radiation from the observation tower at 140 m, downward shortwave radiation (solid black
805 line; W m^{-2}), upward shortwave radiation (dashed black line; W m^{-2}), downward longwave
806 radiation (solid blue line; W m^{-2}), upward longwave radiation (dashed blue line; W m^{-2}), net
807 radiation (red line; W m^{-2}); and (f) sensible heat flux (red line; W m^{-2}) and latent heat flux (red
808 line; W m^{-2}).



809

810

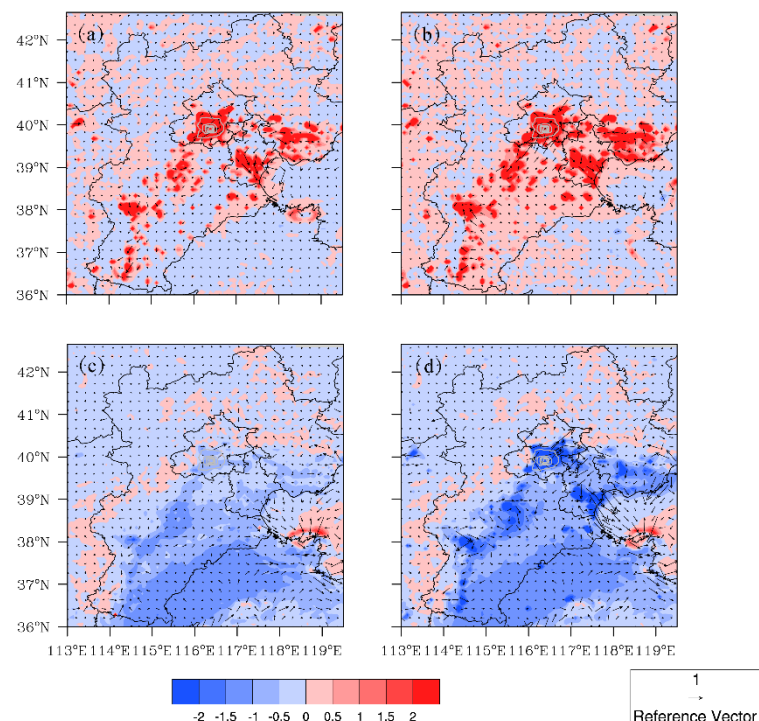
811 Figure 6 Diurnal patterns of simulated variables from the 15th to 23rd of December. (a)
 812 Temperature at 2 m ($^{\circ}\text{C}$); (b) specific humidity (g kg^{-1}) at 2 m; (c) shortwave radiation (W m^{-2});
 813 (d) longwave radiation (W m^{-2}); (e) MLH (m); (f) sensible heat flux (W m^{-2}); and (g) latent heat
 814 flux (W m^{-2}).
 815



816

817 Figure 7 Spatial distribution of the observed concentration of PM_{2.5} (dots; ug m⁻³) and wind field
 818 (vector; m s⁻¹) for two increasing processes of the concentration of PM_{2.5}.

819



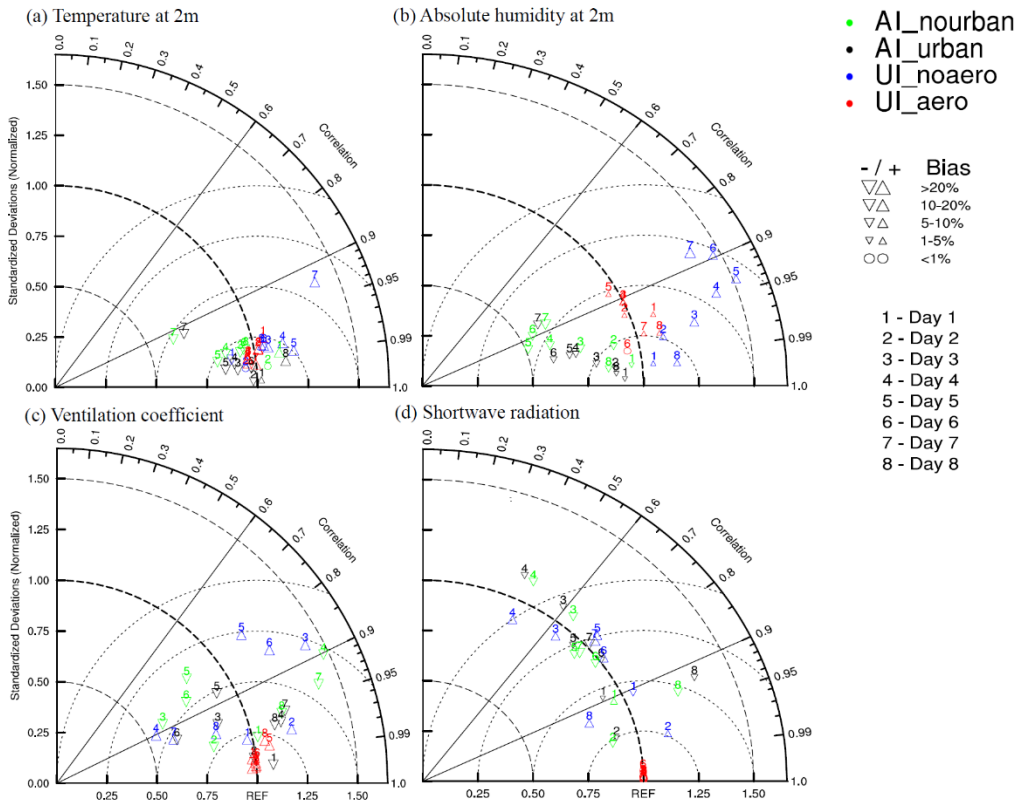
820

821 Figure 8 Spatial distribution of simulated temperature (shading; °C) and wind field (vector; m s⁻¹).
 822 (a) UI_aero; (b) UI_noaero; (c) AI_urban; (d) AI_nourban.

823

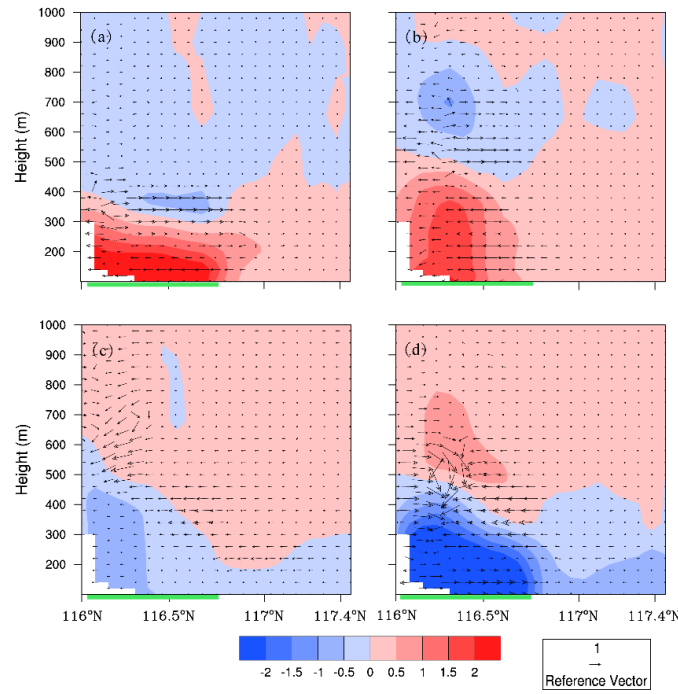
824

825



826

827 Figure 9 Daily means of the four types of impacts (UI_aero, UI_noaero, AI_urban, AI_nourban) in
 828 the eight days are shown in Taylor diagrams in the Beijing area. (a) Temperature at 2 m (°C); (b)
 829 absolute humidity (g kg^{-1}); (c) ventilation coefficient ($\text{m}^2 \text{ s}^{-1}$); (d) shortwave radiation (W m^{-2}).
 830
 831



832

833

834 Figure 10 Cross section at 39.9 °N of average temperature (shading; °C) and wind field (vector; $m s^{-1}$)
 835 from 0000 LST to 0800 LST on the 16th to 20th. (a) UI_aero; (b) UI_noaero; (c) AI_urban; (d)
 836 AI_nourban.

837

838

839

840

841

842

843